WIRELESS COMMUNICATIONS AND MOBILE COMPUTING
Wirel. Commun. Mob. Comput. 2012; **12**:1685–1696
Published online in Wiley Online Library (wileyonlinelibrary.com). DOI: 10.1002/wcm.2339

SPECIAL ISSUE PAPER

Resource allocation with interference mitigation in femtocellular networks

Najah Abu Ali[1]*, Mahmoud Ouda[2], Hossam Hassanein[2] and Osama Kubbar[3]

[1] Faculty of IT, United Arab Emirates University, Al-Ain, United Arab Emirates
[2] School of Computing, Queen's University, Kingston, Canada
[3] Qatar Mobility Innovation Center, Qatar University, Doha, Qatar

ABSTRACT

The introduction of femtocells enabled high data rates and better indoor coverage without the need for expanding or increasing the density of cellular networks deployment or upgrading the cellular network infrastructure. Despite this direct advantage, the introduction of femtocells challenges traditional interference mechanisms because of the ad hoc and dense nature of femtocell deployment. In this paper, we propose an optimal downlink frequency assignment scheme. The proposed algorithm is modeled as a transportation problem to optimally allocate frequency subcarriers with the objective of maximizing the system capacity. The scheme can be used as a benchmark for assessing the suitability of interference mitigation schemes in femtocellular networks. Copyright © 2012 John Wiley & Sons, Ltd.

KEYWORDS

femtocell; radio resource management; interference; OFDMA

***Correspondence**

Najah Abu Ali, Faculty of IT, United Arab Emirates University, Al-Ain, United Arab Emirates.
E-mail: najah@uaeu.ac.ae

1. INTRODUCTION

The introduction of femtocells targeted failing performance of indoor coverage and capacity in pre-4G networks. The importance of indoor coverage emerges as approximately two-thirds of calls, and over 90% of data services occur indoors [1], whereas 45% of households and 30% of businesses experience poor indoor coverage [2]. Mobile operators were thus forced to respond to such serious need to provide a reliable and strong indoor coverage of voice, video, and high-speed data services to meet the ever-increasing traffic demand.

Femtocells are considered a cost-effective solution, which can provide high-quality services and are expected to substantially reduce the operator's cost [3,4] by offloading a significant amount of traffic to indoor spaces, freeing resources at the macrocells and helping outdoor users to receive an enhanced user experience. This offloading is also beneficial for indoor users; no special equipment or upgrades to current handsets are needed to operate the cells apart from the availability of the femtocell base stations (FBSs) [5].

Despite these advantages, networks deploying femtocells face varying types and levels of interference [6]. Typically, an FBS is meant to be operated autonomously and be independently installed by the average user, with little to no technical assistance from the operator. Such autonomy in operation and deployment, however, results in ad hoc and possibly very dense deployment scenarios that challenge traditional schemes utilized for designing and managing interference levels in cellular networks. Such high levels may render the network inefficient and sometimes unusable [7,8].

1.1. Defining interference types

Interference occurs when two or more devices are transmitting 'near' each other. The definition of 'near' describes devices that share one or more communication dimensions, for example, frequency, time, space, or code. The wireless medium faces different types of interference. For example, inter-symbol interference occurs when a symbol overlaps with succeeding symbols because of a delayed multi-path signal. Meanwhile, inter-carrier interference is the distortion of a carrier with other carriers. Co-channel interference occurs when a device transmits on the same channel being used by a nearby device, and adjacent

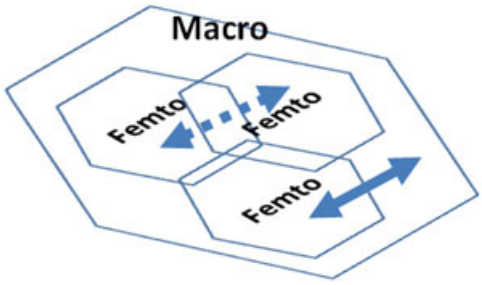

Figure 1. Interference types in a femtocell environment: the dashed line shows co-layer interference, and the solid line shows cross-layer interference.

channel interference arises when signals from a device transmitting on a certain channel jam the transmission of another device on another channel.

Femtocell BSs are to be installed indoors to cover smaller areas when compared with traditional macrocells. Femtocells will always be overlaid on macrocells, unless deployed in remote areas, rendering such deployments as a two-tiered cell composed of a macro-tier and a femto-tier. This tiered deployment is vulnerable to cross-layer interference [1,6,9] where allocations at the macrocellular tier would affect the femtocellular one or vice versa. Co-layer interference might also occur between two cells within the same layer as shown in Figure 1.

Cross-layer interference can be significantly reduced by partitioning the available spectrum between the macrocellular and the femtocellular layers. However, this setup is considered less efficient and limits the amount of spectrum available for each layer [10]. The spectrum can be shared between the two layers, resulting in larger system capacity but rendering the system more vulnerable to interference. In [11], the authors proposed a hybrid spectrum-sharing technique to achieve lower interference and higher capacity system simultaneously. Conversely, co-layer interference can be mitigated using proper frequency allocation and scheduling techniques, or dynamic power adjustment.

1.2. Contribution

As illustrated in Section 2, several works have addressed the specific challenges introduced by femtocells. To the best of our knowledge, however, there remains a need for an optimal solution that is practically implementable. Our intent therefore in this paper is to illustrate the viability of this objective through providing an optimal frequency allocation scheme. The offered scheme is evaluated against two representative schemes.

1.3. Paper organization

The paper is organized as follows. A review of the related work is presented in the next section. In Section 3, a description of the system model and a problem definition are offered, together with a numerical example that illustrates how the proposed scheme works. The setup of the simulation environment utilized in evaluation is detailed in Section 4, with the simulation results presented and discussed in Section 5. Remarks on complexity are made in Section 6. Finally, conclusions are noted.

2. RELATED WORK

Different studies have recently addressed interference mitigation in networks employing femtocells.

In [12], the authors advocate the importance of distributed, self-optimizing schemes because locations and the number of FBSs exhibit a high level of uncertainty. In the scheme, each user has a quality-of-service constraint in the form of a threshold signal-to-interference-and-noise ratio (SINR) for a given service with the objective of meeting the required SINR at each user. The problem is modeled as a linear programming problem and solved using particle swarm optimization, which is an example of a swarm intelligence approach. In a more general context, many have been sought, as swarm intelligence techniques exhibit a communal behavior of self-organizing entities in a distributed environment, such as the ones found in ant colonies and animal herds. The proposed algorithm yields sub-optimal solutions on each femtocell. A heuristic sacrificial mechanism is employed when no feasible solution is available to defer some users' transmissions, causing high interference on the basis of the users' nominal SINR. The algorithm is based on heuristics and takes into account the femtocellular layer only. It involves a significant amount of signaling in favor of being decentralized.

Two reuse partitioning schemes are suggested in [13]. The schemes are applied on overlaid or multiple-layered networks mainly involving the adaptation of cluster size to maintain high signal-to-interference ratio and applying channel assignment. Each hexagonal cell can be viewed as a set of concentric hexagonal cells, each with a different radius.

The schemes proposed were maximal dynamic reuse partitioning and optimal dynamic reuse partitioning. In maximal dynamic reuse partitioning, unused channels are assigned to the innermost region, thus optimizing effective capacity from the subject cell. Meanwhile, in optimal dynamic reuse partitioning, the system allocates unused channels in line with the areas and the distribution of users within the concentric signal-to-interference-ratio regions to maintain a certain grade of service. The adaptive nature of the proposed schemes makes them more powerful when compared with similar schemes.

The work in [14] studies the mitigation of downlink femto-to-macro interference through dynamic resource partitioning. The system is an Orthogonal Frequency Division Multiple Access (OFDMA) two-tiered network that uses universal frequency reuse. The transmission power of a 3GPP BS, called eNode B, is more than

that of a home eNode B, a femtocell within 3GPP context. Such difference makes it more likely that macrocell user equipment (MUE) within the transmission range of femtocells will cause interference to the surrounding user equipment (UE) and experience low SINR. The authors suggest prohibiting home eNode B from accessing downlink resources that are assigned to neighboring MUE to preserve universal frequency reuse. The interference to the most vulnerable MUE is then effectively controlled at the cost of sacrificing a minor portion of the femtocell capacity. The study is based on the assumption that compromising some femtocell resources will lead to a better system throughput.

The authors in [15] propose a greedy-based dynamic frequency assignment scheme by assigning the quietest channels, that is, the ones least frequently utilized, to femtocells according to the received power level. The algorithm proceeds in two stages. First, each FBS scans the entire spectrum and selects the frequency bandwidth that describes the lowest received power level. Next, each FBS measures and sorts the received power level on every subchannel of its frequency bandwidth and assigns the quietest sub-channels to its UE. The algorithm works in a decentralized manner fast and without complexity but may not yield significant results when compared with other algorithms in the field.

A scheme exploiting coverage adaptation through balancing FBSs transmission powers is offered in [16]. Power control decisions are made according to the available mobility information about the surrounding users. The purpose is avoiding pilot signal leakage outside a house, which may lead to increasing mobility events or decreasing power significantly resulting in the same outcome. The study is considered a contribution to the auto-configuration and self-optimization aspects in femtocell networks. The paper distinguishes between auto-configuration and self-optimization but allocating the former responsibility for initially configuring the FBS, whereas the self-optimization is concerned with enhancing the current configuration during the femtocell network operation.

In [17], the authors present the capacity–interference tradeoff in a two-tier environment comparing using shared bandwidth and dedicated bandwidth. The proposed scheme divides the area around a macrocell into inner and outer regions. An FBS within the inner region will not operate in a co-channel mode (shared bandwidth) to avoid interference. It instead uses a frequency band other than that used by the macrocell base station (MBS). The authors attempt to find the best threshold that splits the two regions. Interference limited coverage area is derived by estimating power levels using different path-loss models.

The effect of two power control schemes were studied in [18]. The schemes are geo-static power control and adaptive power control. In the first schemed, called geo-static power control, the transmitted power of a femtocell is based on its distance from the macrocell. Meanwhile, in adaptive power control, the transmitted power of femtocells are adjusted on the basis of the network target rates, thus enhancing the femtocell users' throughput without compromising performance.

The problem of distributed power control in femtocells is modeled as a non-coperative game in [19]. In the game, each FBS determines the trasmit power with the maximum benefit. The system considers fairness; femtocells serving more mobile stations are allowed to transmit at higher power levels to maintain service to its users. A payoff function based on revenue and cost was derived, where the cost is directly proportional with the transmission power to advise FBSs to reduce their transmission powers. Transmission powers reach Nash equilibrium (steady state) in the simulated game. Game theory has been also used in other femtocell interference mitigation related studies [20,21].

In [3], the authors study a centralized radio resource management for femtocell dense deployment and derive an objective function to maximize the system capacity. The problem was divided into two parts: sub-channel allocation and power allocation. The authors in [22] advocate the prevention of the usage of some frequencies by a femtocell if they are already assigned to a near MUE. Availability of macrocell frequency scheduling information is assumed.

Table I offers a comparison of the aforementioned works surveyed and illustrates the persisting need for an optimal solution that (1) attends to the specific nature of resource allocations in OFDMA networks, (2) mitigates interference in networks employing femtocells in an optimal fashion, and (3) considers both the femtocellular and the macrocellular tiers. On the basis of the aforementioned representative schemes from literature, it can be inferred that optimized solutions are not fully realized.

3. SYSTEM DESCRIPTION AND MODEL

We consider an OFDMA network with two layers: femtocellular and macrocellular. The macrocellular layer is the traditional layer in the cellular network, which encompasses MBSs deployed at specific cell sites, whereas the femtocellular layer consists of several shorter range cells resulting from the deployment of FBSs in an ad-hoc manner. Each BS has a number of UE to serve. UE that belong to the femtocellular layer, that is, connected to FBSs, are referred to as femtocell user equipment (FUE), whereas UE connected to an MBS are referred to as macrocell user equipment (MUE). UE are served in units of resource blocks (RBs). In OFDMA downlink, an RB is a basic time-frequency unit. It consists of 12 consecutive subcarriers in the frequency domain and seven OFDM symbols in the time domain, assuming normal cyclic prefix. The minimum unit to serve a UE is an RB; that is, a user is either admitted access to a whole RB or not. The problem investigated in this work is the assignment of RBs among system users. An optimal assignment algorithm is proposed, aimed at maximizing the system capacity.

Table I. Comparison of recent interference mitigation studies.

Scheme	Direction	Locality	Technique	Optimization method
[12]	Downlink	Decentralized	Power control, frequency scheduling	Particle swarm optimization and heuristics
[13]	N/a	Decentralized	Channel allocation	N/a
[14]	Downlink	Decentralized	Spectrum partitioning	N/a
[15]	Downlink	Decentralized	Frequency planning, frequency assignment	Greedy based
[16]	N/a	Decentralized	Power control	Feedback-based iterative optimization
[17]	Downlink	Centralized	Frequency planning	N/a
[18]	N/a	Decentralized	Power control	Feedback-based iterative optimization
[19]	N/a	Decentralized	Power control	Game theory
[3]	Downlink	Centralized	Sub-channel allocation	Iterative optimization

3.1. Problem definition

Given L mixed—femto and macro—BSs labeled 1 through L, let U_j be the number of UE associated with BS j, where $1 \leq j \leq L$. For each cell, one can measure the SINR for each UE per each RB. This can be arranged in a matrix $S_{U_j,R}$ where R is the number of RBs in the accessible spectrum. Each entry in this matrix signifies the SINR that a UE will experience when assigned a specific RB as calculated in [23].

All resulting SINR matrices of all BSs are aggregated into one matrix $\Gamma_{U,R}$ by adding the rows representing the UE into the matrix. Let $\gamma_{u,r}$ be an entry in Γ, it represents the SINR that UE u, $(1 \leq u \leq U)$, will experience if assigned RB r, $(1 \leq r \leq R)$.

Let $\omega_{u,r}$ be a binary output function indicating whether an RB r is assigned to a UE u or not, such that $\omega_{u,r} = 1$ if RB r is assigned to UE u and 0 otherwise.

The proposed algorithm maximizes the summation of the chosen SINR values as follows:

$$\sum_{u=1}^{U} \sum_{r=1}^{R} \omega_{u,r} \cdot \gamma_{u,r} \tag{1}$$

Subject to constraint:

$$\sum_{\forall u} \omega_{u,r} \in \{0, 1\} \tag{2}$$

The objective function in expression 1 indicates that the summation of SINR of all assigned RBs is to be maximized, whereas the only constraint in expression 2 means that an RB will be assigned to at most one UE.

3.2. Proposed solution approach

The problem of assigning RBs to UE can be modeled as a transportation problem [24]. In a transportation problem, a set of graph nodes N is partitioned into two subsets U and V (not necessarily of equal cardinality) such that as follows:

(1) Each node in U is a supply node.
(2) Each node in V is a demand node.
(3) A set of edges running between the two subsets exist. Each edge (i, j) joins a node $i \in U$ with a node $j \in V$.

U represents the demand nodes, and V represents the supply nodes. Link (i, j) means that a node i is supplied via node j. Note that the two subsets U and V are disjoint. Accordingly, the ordering of sets does not matter, and edges that run between subsets can still be modeled as directed edges.

A generic modeling of this problem is a bipartite graph as shown in Figure 2, with two disjoint sets U and V. Minimum cost flow (MCF) gives the optimal solution to a network visualized as a directed weighted graph. The optimal solution represents a set of edges chosen that results in the minimization of the sum of their weights/costs. Given the SINR matrix Γ, the problem can be visualized as a directed graph with two disjoint sets of

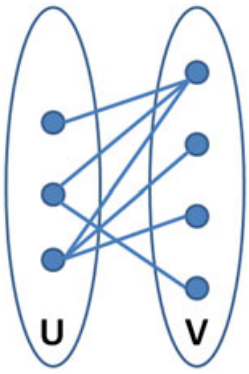

Figure 2. Example of a bipartite graph.

nodes representing UE and RBs, U and V, respectively. Graph edges originate from nodes in U to nodes in V, and the cost of a link between node $i \in U$ and node $j \in V$ equals $\gamma_{u,r}$. It can be seen how the matrix in Figure 3 can be mapped to the directed graph in Figure 4. Because a typical MCF problem calculates the flow between a single source and a sink, an artificial source preceding all nodes in U and an artificial sink following all nodes in V were added as shown in Figure 5. Links from/to the artificial source/sink are of zero cost, in order not to affect the calculations. For each BS, the SINR values for all its UE against all available RBs are evaluated. All the resulting matrices are aggregated into one matrix of all UE per each RB. The matrix is then converted to a directed graph and solved via MCF. The resulting assignment will highlight edges that give the maximum summation of the SINR values on these edges after running the algorithm, thus making it one of the possible optimal assignments. The following subsection presents a numerical example to clarify the proposed scheme.

$$\begin{matrix} \gamma 1,1 & \gamma 1,2 & \cdots & \cdots & \gamma 1,R \\ \gamma 2,1 & \gamma 2,2 & & & \gamma 2,R \\ \vdots & & \ddots & & \vdots \\ \vdots & & & \ddots & \vdots \\ \gamma U,1 & \gamma U,2 & \cdots & \cdots & \gamma U,R \end{matrix}$$

Figure 3. Example of signal-to-interference-and-noise-ratio matrix.

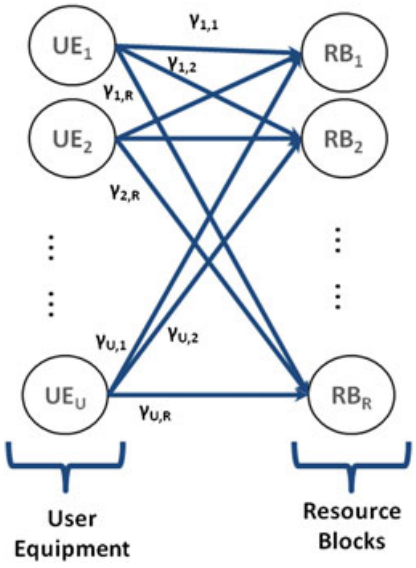

Figure 4. Mapping signal-to-interference-and-noise-ratio matrix to a bipartite graph.

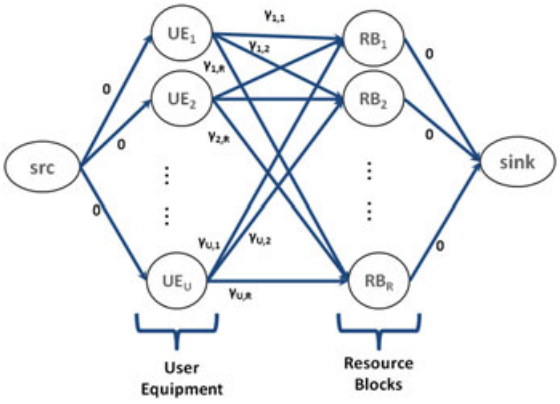

Figure 5. Bipartite graph after adding artificial source and sink.

3.3. A numerical example

We define two sets $\mathbb{A} = \{A, B, C\}$ and $\mathbb{B} = \{1, 2, 3, 4, 5, 6, 7\}$. The goal is to assign exactly two nodes from set $\mathbb{B}$ to one node from set $\mathbb{A}$ such that the total summation of the assigned values is minimized. The costs of assigning a node from set $\mathbb{B}$ to a node from set $\mathbb{A}$ are given in an adjacency matrix, as shown in Table II.

Table III shows how the optimal solution should look like. The adjacency matrix described earlier is repeated, and the bold values indicate the values that have been chosen for the optimal assignment. For example, nodes 3 and 4 are assigned to node A.

Note that the algorithm is not a greedy-based algorithm. For example, the least two interference values in the given matrix, 0.0000 and 0.023, were not chosen in the optimal solution. Similarly, the least interference value for row B (0.0232) was not chosen, and the least interference value for column 7 (0.000) was not chosen as well. Choosing any of these will lead to a higher global cost. Additionally, the resulting summation (1.633) is the *global least value* of all solutions that can be achieved given the problem constraints (two nodes from set $\mathbb{B}$ should be associated to a node from set $\mathbb{A}$). Hence, the algorithm proposed results in an optimal solution.

Table II. Numerical example: adjacency matrix.

	1	2	3	4	5	6	7
A	0.378	0.245	0.174	0.379	0.839	0.632	0.000
B	0.341	0.971	0.293	0.560	0.717	0.197	0.023
C	0.481	0.432	0.766	0.799	0.821	0.440	0.110

Table III. Numerical example: adjacency matrix optimal solution.

	1	2	3	4	5	6	7
A	0.378	0.245	**0.174**	**0.379**	0.839	0.632	0.000
B	**0.341**	0.971	0.293	0.560	0.717	**0.197**	0.023
C	0.481	**0.432**	0.766	0.799	0.821	0.440	**0.110**

3.4. The minimum cost maximum flow algorithm

The MCF algorithm runs in one loop. In each iteration, a call to a shortest-path algorithm takes place, finding the shortest path from the source to the sink. This path is 'augmented' to the current solution; that is, the flows on the links along this path are subtracted from the capacities on these links and added to the capacities of the reverse edges. Note that each edge has a negative cost of the reverse edge; this allows us to 'rollback' or trade some of the already assigned flows. Algorithm 1 keeps on augmenting paths (by calling getPath method) until the total augmented flow is zero—in this case, the algorithm terminates. Augmenting a path subtracts a number of flow units from all edges on this path and adds the same number of flow units to the reverse path; this helps rerouting when necessary and prevents the algorithm from recalculating an already established path.

Algorithm 1 Minimum cost maximum flow algorithm.

```
1:  while true do
2:      getPath(vertices, edges, source) {Call Bellmanford
        shortest path}
3:      pathflow ← dest.flow
4:      if pathflow = 0 then
5:          return
6:      end if
7:      current ← sink
8:      while current ≠ source do
9:          se.capacity ← se.capacity − pathflow {let
            se be the directed edge from current.parent to
            current}
10:         rev.capacity ← rev.capacity + pathflow
            {let rev be the reverse edge of se}
11:         current ← current.parent
12:     end while
13: end while
```

4. SIMULATION SETUP

The system simulated consists of a two-tiered OFDMA network composed of a macro-tier and femto-tier. The macro-tier encompasses a sole macrocell and a number of macrocell users. Similarly, The femto-tier consists of a number of femtocells and their respective users. Figure 6 shows the network layout of the simulated environment.

The frequency planning model used in the simulation is co-channel allocation where a certain frequency band is shared between the femto-tier and the macro-tier. This setup is adopted by operators who seek larger system capacity and can tolerate more interference in their networks. The frequency band is split into a number of subcarriers, which are grouped together to form RBs. RBs are considered the smallest units that a UE can obtain in terms of frequency allocation. The core of the simulation is based on the SINR experienced by every UE at each RB. SINR generation is based on the model proposed in [23] where a closed-form modeling for the downlink SINR is presented. Using the antenna gains of a BS and a UE connected to it, transmission power of the BS and locations of interfering BSs as well as location of the UE, the authors have derived a probability density function for the downlink SINR conditioned on the location of a UE within a femtocell. Table IV shows the simulation parameters used in all experiments.

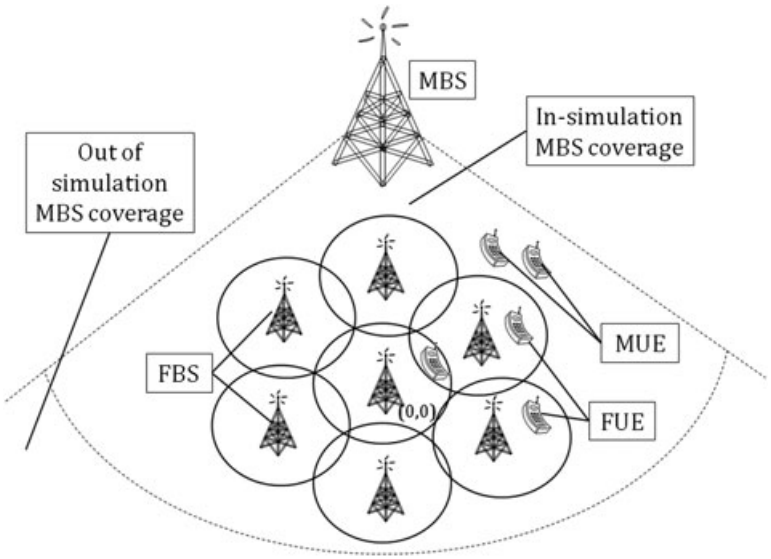

Figure 6. Physical layout of the simulated environment. MBS, macrocell base station; FBS, femtocell base station; MUE, macrocell user equipment; FUE, femtocell user equipment.

Table IV. General simulation parameters.

Parameter	Symbol	Value
Antenna gain of BS	G_b	3 dBi
Antenna gain of MS	G_m	0 dBi
Constant of path loss	C_s	43.8 dB
Path-loss exponent on the link between a BS and a MS	α_j	3.6
MS noise figure	φ	7 dB
Channel bandwidth	W	10 MHz
Central frequency	f	5.25 GHz
Ambient temperature	T	293 K
Number of subcarriers per resource block	N_{SC}	12
Number of resource blocks	N_{RB}	50
Number of femtocells	N_f	2–7
Number of users per femtocell j	N_{f_j}	3–5
Number of macrocell users	N_m	10–20
Transmission power of femtocell j	P_j	10–30 dBm
Transmission power of macrocell	P_m	43-46 dBm
Variance of shadow fading	σ_{X_s}	1–4
Distance between user i and femtocell j	D_{ij}	1–30 m
Distance between femtocell j and the center femtocell	D_j	10–50 m
Distance between the macrocell and the center femtocell	D_m	100–300 m
Distance between user i and the macrocell	D_{im}	50–200 m
Adjusting factor	β	ln(10)/10

BS, base station; MS, message service.

Two representative schemes are chosen to evaluate the performance of the proposed algorithm. The first is proposed by Kim *et al*. in [3] and is a centralized system capacity maximization algorithm. The algorithm proceeds in two phases: power allocation and sub-channel allocation. To match the objective function of this scheme with the proposed MCF, only the sub-channel allocation part has been implemented. To maintain the simulation assumptions in [23], transmission power of a BS is kept constant throughout a single experiment. Two versions of this algorithm have been developed; a closed subscriber group (CSG) version, to match the simulation assumptions for the proposed MCF algorithm, and another open subscriber group (OSG) version, to fully exploit the strength of Kim's algorithm. The difference between the two versions is that in a CSG environment, users are pre-attached to their BSs, and hence, users are allocated RBs at the serving BS, whereas in the OSG version, a UE is allowed to switch to a better serving BS by means of handover. The OSG version is referred to as Kim09OSG, and the CSG version is referred to as Kim09CSG. Algorithm 2 shows the CSG of Kim's algorithm (Kim09CSG).

The second algorithm is an in-house greedy algorithm and is used in evaluating the performance of the proposed MCF. The greedy algorithm has the same SINR matrix with the MCF as input. It starts by sorting all the values in the matrix in a descending order. And given the number of RB required by each UE, the algorithm starts looking up SINR values from the top to bottom, maintaining the condition that no two UE share an RB, and keeps assigning RBs to UE until each UE gets its required RBs. Algorithm 3 shows a pseudo-code for the in-house greedy algorithm.

Algorithm 2 Kim09CSG algorithm.

1: Let $rate$ be the required user rate in units of RBs.
2: Let $\Gamma_{N,R}$ be the SINR matrix of N UE versus R RBs.
3: Let $allocated$ be an integer array of size N.
4: **for all** r **do**
5: Find the best $\gamma_{n,r} \in \Gamma$ where $allocated[n] < rate$
6: $allocated[n] \leftarrow allocated[n] + 1$ {Assign RB r to UE n}
7: **end for**

5. SIMULATION RESULTS

System capacity is chosen to be the performance evaluation metric. Capacity is regarded as the achievable theoretical system throughput given a certain assignment of RBs to UE. Capacity C for an assignment is calculated as $B \sum_{r} \sum_{p=1}^{P} \log_2(1 + \gamma_{rp})$ where B is the physical bandwidth, r is an RB assigned to a user, P is the number of subcarriers per RB, and γ_{rp} is the SINR of the pth subcarrier in RB r.

5.1. Effect of changing number of users per femtocell

In this experiment, capacity is evaluated in response to changing the number of users per femtocell. The

Algorithm 3 In-house greedy algorithm.

Let $rate$ be the required user rate in units of RBs.
Let $\Gamma_{N,R}$ be the SINR matrix of N UE versus R RBs.
Let $allocated$ be an integer array of size N.
Let $booked$ be a boolean array of size R.
sort(Γ) {Sort the SINR matrix in descending order}
for all n **do**
  $allocated[n] \leftarrow 0$
end for
for all r **do**
  $booked[r] \leftarrow false$
end for
for all $\gamma_{n,r}$ in Γ **do**
  if $allocated[n] < rate$ and $booked[r] = false$ **then**
    $allocated[n] \leftarrow allocated[n] + 1$ {Assign RB r to UE n}
    $booked[r] \leftarrow true$ {Mark RB r as used}
  end if
end for

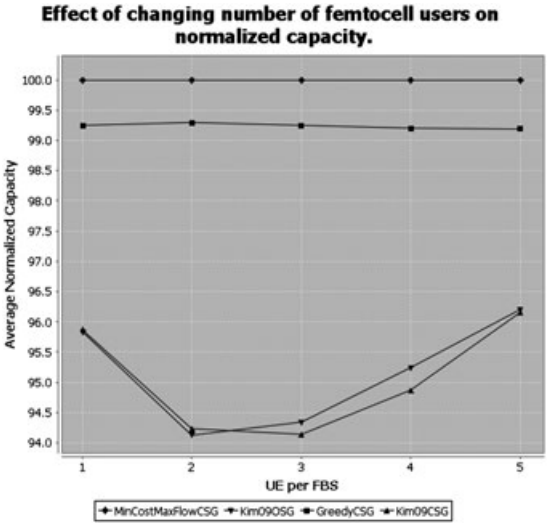

Figure 7. Average normalized capacity versus changing number of users per femtocell. UE, user equipment; FBS, femtocell base station.

experiment has been repeated 20 times for each value from the set [1, 2, 3, 4, 5]. For each experiment run with a certain seed, all capacities attained from all schemes are normalized relative to 100, i.e., the capacity value of the algorithm that scores best is set to 100, and capacities from other algorithms are set to a percentage of the best capacity, as in equation (3). Then, for each value of N_{f_j}, all normalized capacities are averaged as in equation (4)

$$\text{Normalized capacity at seed } s = \frac{\text{Capacity at seed } s}{\text{Best capacity at seed } s} * 100 \tag{3}$$

$$\text{Normalized capacity at a certain value } N_{f_j} = \frac{\sum_s \text{Normalized capacity at seed } s}{20} \tag{4}$$

Figure 7 shows the simulation results of the experiment. The proposed optimal algorithm, MCF, outperforms all other schemes as expected. The in-house greedy approach scores near-optimal capacity, 0.5% to 1.0% less performance than optimal. Kim09OSG and Kim09CSG scored alternating results at 3.5% to 6.0% less performance than optimal. The near-optimal performance of the in-house greedy approach can be attributed to the data distribution of SINR values. A UE will experience slightly varying SINR values per each RB. Hence, choosing greedily to assign a certain RB to a UE will not incur a significantly large cost in terms of blocking another UE to use the same RB if it results in a total higher capacity.

5.2. Effect of changing the total number of serving femtocell access points)

In this experiment, capacity is evaluated against changing the total number of serving femtocells, while keeping the number of users constant. The total number of femtocell users is split equally among the number of femtocells. The experiment has been repeated 20 times per each value from the set [1, 2, 3, 4]. Capacities of all algorithms are calculated and normalized per each seed value.

The results of the experiment are shown in Figure 8. MCF still outperforms the other schemes. The in-house greedy approach comes next at 99% to 99.5% optimal performance, whereas Kim09OSG and Kim09CSG scored alternating results at 95% to 97.5% optimal performance.

5.3. Effect of user mobility

In this experiment, capacity is calculated to assess the effect of user mobility on the performance of the algorithms under investigation. A simple random waypoint mobility model was applied. Across the interval of 50 iterations, each UE may randomly move to another position. The new position can be 1 m away in the horizontal direction, and/or 1 m away in the vertical direction from the old position. The number of FUE simulated in this experiment is 16, and the number of MUE is 9, for a total of 25 UE. This results in two RBs per user.

The layout generation is performed once at the beginning of this experiment. The positions of all UE are updated at each iteration by applying random waypoint mobility model. The SINR matrix is calculated at each

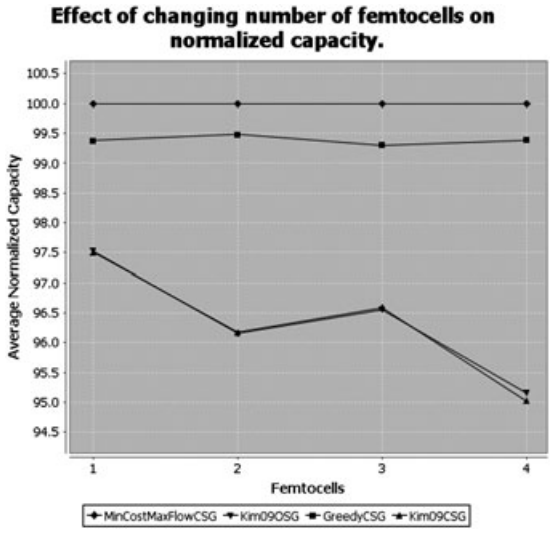

Figure 8. Average normalized capacity versus changing number of femtocells.

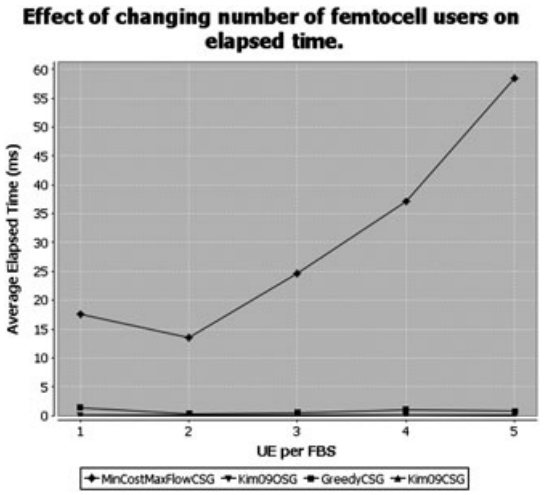

Figure 10. Average elapsed time. UE, user equipment; FBS, femtocell base station.

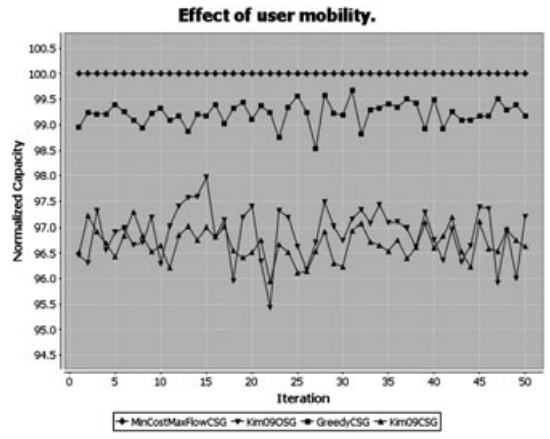

Figure 9. Effect of applying random waypoint mobility model on the normalized capacity.

iteration before the algorithms run again for this iteration. The results of the experiment are shown in Figure 9. The proposed benchmark MCF stays at the top, whereas the in-house greedy approach is just below it at 98.5% to 99.7% optimal performance. Kim09OSG and Kim09CSG fluctuate around 95.5% to 98% optimal performance.

5.4. Elapsed time

To further elaborate on the practicality of the proposed solution and the other schemes, we repeated the experiment in Section 5.1 to study the elapsed time. The elapsed time is the total simulation time for each experiment recorded in milliseconds and averaged per user value N_{f_j} as shown in Figure 10. Section 6 provides complexity analysis as a means of supporting the elapsed time results.

Clearly, the optimal MCF takes more time undergoing calculations to achieve optimality. The in-house greedy scheme comes in the second place with much lower complexity and time, whereas the two versions of Kim's algorithm score the best performance because of their relatively low complex nature.

In the aforementioned experiments, a greedy scheme performed significantly well when compared with the optimal scheme, whereas the other two approaches, Kim09OSG and Kim09CSG, did not achieve a similar performance. The main drawback in Kim's approach proposed in [3] is that it deals with one RB at a time, trying to maximize the benefit (capacity) from using this RB. The problem is that a UE can be sufficiently served from earlier RBs, thus alienating better capacity RBs that might come later and wasting good RBs on other UE. This flaw in Kim's approach did not let it benefit fully from being a greedy-based scheme.

6. REMARKS ON SOLUTION COMPLEXITY

The proposed algorithm runs in iterations. It finds the shortest path in every iteration, assigning an RB to a user, possibly reassigning another RB if needed. To calculate the runtime complexity, define N as the total number of UE, including FUE and MUE, and let R be the total number of RBs available; hence, the outer loop complexity is $O(R)$. The call to Bellmanford shortest path depicted in Algorithm 1 has a worst-case complexity of $O(V \cdot E)$ where V is the size of $vertices$ list and E is the size of $edges$ list. Because the generated graph is fully connected then $V = R + N + 2$ and $E = R \cdot N + R + N$. Essentially, this comes from R RBs; each one is connected to N UE,

Table V. Complexity analysis of the algorithms in simulation.

Algorithm	Complexity	Average runtime (ms)
MCF	$O(R^3 \cdot N + R^2 \cdot N^2)$	10s of ms
In-house greedy	$O(N \cdot R \cdot \log(N \cdot R))$	1 ms
Kim09CSG	$O(R \cdot N)$	< 1 ms

in addition to N links to the artificial source and R links to the artificial sink. Note that the dominant term is $R \cdot N$. Hence, the total complexity of an MCF based on Bellmanford shortest path is $O(R \cdot (R + N) \cdot (R \cdot N)) = O(R^2 \cdot N(R + N))$.

Algorithm 2 encompasses R loops on all RBs; each has a maximum of N UE to check. This brings the algorithm to a complexity of $O(N \cdot R)$. Similarly, the OSG version of this algorithm, referred to as Kim09OSG, is $O(N \cdot R \cdot B)$, where B is the number of BSs.

The greedy algorithm 3 starts by sorting out the SINR matrix, typically with complexity $O(N \cdot R) \log(N \cdot R)$. The loop in lines 11–17 is of $O(N \cdot R)$. Because sorting is the dominating factor, the algorithm complexity is of $O(N \cdot R) \log(N \cdot R)$. Table V summaries the complexity analysis of the three algorithms.

The achieved results may not justify the MCF complexity, despite the fact that it is optimal and the running time is reasonable. We would like to note that the achieved results are affected by the value of the SINR of the RB generated on the basis of the analysis presented in [23], because the allocated RB per user in our simulation have comparable SINR values. However, lab simulations of MCF have proven that in cases where SINR values differ greatly per UE (the SINR is cusomly generated not following [23]), the performance gain was as high as 50%, according to the discrepancy in SINR levels.

7. CONCLUSIONS

We proposed a resource allocation algorithm for OFDMA femtocells, which mitigates interference at the two network tier levels: the femto–femto tier and the femto–macro tier. The proposed algorithm is modeled as a transportation problem to optimally allocate frequency subcarriers with the objective of maximizing the system capacity. The proposed algorithm can serve as an optimized benchmark for allocating frequency RBs in OFDMA femtocell network or as a benchmark to evaluate heuristic or sub-optimal frequency assignment schemes proposed in literature.

ACKNOWLEDGEMENT

This work was made possible by a National Priorities Research Program (NPRP) grant from the Qatar National Research Fund (Member of Qatar Foundation).

REFERENCES

1. Zhang J, De La Roche G, La De Roche G. *Femtocells: Technologies and Deployment*. John Wiley and Sons, Ltd.: Chichester, UK, 2010.
2. Cullen J. *Radioframe presentation*. Femtocells Europe: London, UK, June 2008.
3. Kim JY, Cho D-H. A joint power and subchannel allocation scheme maximizing system capacity in dense femtocell downlink systems, In *2009 IEEE 20th International Symposium on Personal, Indoor and Mobile Radio Communications*, Tokyo, Japan, September 2009; 1381–1385.
4. Knisely D, Yoshizawa T, Favichia F. Standardization of femtocells in 3GPP. *IEEE Communications Magazine* September 2009; **47**(9): 68–75.
5. Yun J-H, Shin KG. Adaptive interference management of OFDMA femtocells for co-channel deployment. *IEEE Journal on Selected Areas in Communications* June 2011; **29**(6): 1225–1241.
6. Cheng S-M, Lien S-Y, Chu F-S, Chen K-C. On exploiting cognitive radio to mitigate interference in macro/femto heterogeneous networks. *IEEE Wireless Communications* June 2011; **18**(3): 40–47.
7. Lopez-Perez D, Guvenc I, de la Roche G, Kountouris M, Quek TQS, Zhang J. Enhanced intercell interference coordination challenges in heterogeneous networks. *IEEE Wireless Communications* June 2011; **18**(3): 22–30.
8. Sundaresan K, Rangarajan S. Efficient resource management in OFDMA femto cells. In *Proceedings of the Tenth ACM International Symposium on Mobile Ad Hoc Networking and Computing*, MobiHoc '09. ACM: New York, NY, USA, 2009; 33–42.
9. Lopez-Perez D, Valcarce A, de La Roche G. OFDMA femtocells: a roadmap on interference avoidance. *IEEE Communications Magazine* September 2009; **47**(9): 41–48.
10. Bai Y, Zhou J, Chen L. Hybrid spectrum usage for overlaying LTE macrocell and femtocell. *GLOBECOM 2009—2009 IEEE Global Telecommunications Conference* 30 November - 04 December 2009; 1–6.
11. Bai Y, Zhou J, Chen L. Hybrid spectrum sharing for coexistence of macrocell and femtocell, In *IEEE International Conference on Communications Technology and Applications, 2009. ICCTA '09*, Beijing, China, October 2009; 162–166.
12. Akbudak T, Czylwik A. Distributed power control and scheduling for decentralized OFDMA networks, In *2010 International ITG Workshop on Smart Antennas (WSA)*, Bremen, Germany, February 2010; 59–65.
13. Aki H, Cenk Erturk M, Arslan H. Dynamic channel allocation schemes for overlay cellular

architectures. In *Proceedings of the 9th Conference on Wireless Telecommunications Symposium*, WTS'10. IEEE Press: Piscataway, NJ, USA, 2010; 67–71.
14. Bharucha Z, Saul A, Auer G, Haas H. Dynamic resource partitioning for downlink femto-to-macro-cell interference avoidance. *EURASIP Journal on Wireless Communications and Networking* January 2010; **2010**: 2:1–2:12.
15. El Mouna Zhioua G, Godlewski P, Hamouda S, Tabbane S. Quietest channel selection for femtocells in OFDMA networks. In *Proceedings of the 8th ACM International Workshop on Mobility Management and Wireless Access*, MobiWac '10. ACM: New York, NY, USA, 2010; 125–128.
16. Claussen H, Ho LTW, Samuel LG. Self-optimization of coverage for femtocell deployments, In *Wireless Telecommunications Symposium, 2008. WTS 2008*, April 2008; 278–285.
17. Guvenc I, Jeong M-R, Watanabe F, Inamura H. A hybrid frequency assignment for femtocells and coverage area analysis for co-channel operation. *IEEE Communications Letters* December 2008; **12**(12): 880–882.
18. Arulselvan N, Ramachandran V, Kalyanasundaram S, Han G. Distributed power control mechanisms for HSDPA femtocells, In *VTC Spring 2009—IEEE 69th Vehicular Technology Conference*, Barcelona, Spain, April 2009; 1–5.
19. Hong EJ, Yun SY, Cho D-H. Decentralized power control scheme in femtocell networks: a game theoretic approach, In *2009 IEEE 20th International Symposium on Personal, Indoor and Mobile Radio Communications*, Tokyo, Japan, September 2009; 415–419.
20. Chen C-W, Wang C-Y, Chao S-L, Wei H-Y. Dance: a game-theoretical femtocell channel exchange mechanism. *ACM SIGMOBILE Mobile Computing and Communications Review* July 2010; **14**: 13–15.
21. Chandrasekhar V, Andrews JG, Muharemovic T, Shen Z, Gatherer A. Power control in two-tier femtocell networks. *IEEE Transactions on Wireless Communications* August 2009; **8**(8): 4316–4328.
22. Sahin ME, Guvenc I, Jeong M-R, Arslan H. Handling CCI and ICI in OFDMA femtocell networks through frequency scheduling. *IEEE Transactions on Consumer Electronics* November 2009; **55**(4): 1936–1944.
23. Sung KW, Haas H, McLaughlin S. A semi-analytical PDF of downlink SINR for femtocell networks. *EURASIP Journal on Wireless Communications and Networking* 2010; **2010**: 1–10.
24. Ahuja RK, Magnanti TL, Orlin JB. *Network Flows: Theory, Algorithms, and Applications*. Prentice Hall: Englewood Cliffs, NJ, 1993.

AUTHORS' BIOGRAPHIES

Najah Abu Ali is currently an associate professor at the college of Information Technology in the United Arab Emirates University. She obtained her PhD degree in Computer Networks from Electrical Engineering Department at Queen's University, Kingston, Canada. Her research interests comprise analytical and measurement-based network performance evaluation and radio resource management of wireless broadband and sensor networks. She published her work in several reputable journals and conferences and delivered several refereed tutorials at reputable conference.

Mahmoud Ouda had his BSc in Computer Science from Cairo University and MSc from the School of Computing at Queen's University. His master thesis titled 'Interference-optimal frequency allocation in femtocellular networks' discussed the applicability to use optimized graph theoretic algorithms in wireless frequency allocation. He worked for IBM Cairo Technology Development Center and is currently holding a software engineering role at Google Inc. His main interests are web security and game programming.

Hossam Hassanein is leading research in the areas of wireless and mobile networks architecture, protocols, and services. His record spans more than 500 publications in journals, conferences, and book chapters, in addition to numerous keynotes and plenary talks in flagship venues. He has received several recognition and best papers awards at top international conferences. He is also the founder and director of the Telecommunications Research Lab at Queen's University School of Computing, with extensive international academic and industrial collaborations. He is a senior member of the IEEE and is a former chair of the IEEE Communication Society Technical Committee on Ad hoc and Sensor Networks. He is an IEEE Communications Society distinguished speaker (distinguished lecturer 2008-2010).

Osama Kubbar received his MSc and PhD degrees from Queen's University, Canada in 1994 and 1998, respectively. He has extensive experience in architecture, design, and performance analysis of telecommunications networks and protocols for wireless and wireline, and currently, he is a system principal architect at QU Wireless Innovation Centre (QUWIC).

His area of expertise is in L2/L3 protocol design and performance analysis. He joined Nortel Network, Canada in August 1998 as a research scientist in the wireless system engineering division and led projects related to the design and performance analysis of MAC protocols, CAC, traffic scheduling and QoS management, radio resource management, and TCP and ARQ/HARQ performance assessment. He also has experience in core network architecture and IP protocols/nodal interfaces. In 2005, he held the role of System Design Authority at Nortel, in which he managed the end-to-end features' design and performance assessment, integration, and testing. His work and expertise span multiple technologies in 2G/3G/4G for 3GPP, 3GPP2, and IEEE such as TDMA, CDMA2000, 1xrTT-DO, 802.11, WiMAX, LTE, and Femtocells. He holds three registered patents with two of them product implemented and many Nortel internal proprietary designs. In June 2008, he joined TruePosition Inc. in the US as a system principal architect and led the system activities in the development and testing of the UMTS Mobile location architecture and software release. In July 2009, he joined QUWIC, where he is leading the development of innovative solutions for multiple market segments, such as telecommunications, oil/gas, and environment.

Wirel. Commun. Mob. Comput. 2012; **12**:1685–1696 © 2012 John Wiley & Sons, Ltd.
DOI: 10.1002/wcm